Climbing Fiber Projections in Relation to Zebrin Stripes in the Ventral Uvula in Pigeons

Janelle M.P. Pakan,[1] David J. Graham,[2,3] and Douglas R. Wylie[2,3]*

[1]Centre for Integrative Physiology, University of Edinburgh, UK
[2]Centre for Neuroscience, University of Alberta, Edmonton, Alberta, Canada, T6G 2E9
[3]Department of Psychology, University of Alberta, Edmonton, Alberta, Canada, T6G 2E9

ABSTRACT

The cerebellum consists of sagittally oriented zones that are delineated by afferent input, Purkinje cell response properties, and the expression of molecular markers such as zebrin II (ZII). ZII is heterogeneously expressed in Purkinje cells such that there are parasagittal stripes of high expression (ZII+) interdigitated with stripes of little or no expression (ZII−). In pigeons, folium IXcd consists of seven pairs of ZII+/− stripes denoted P1+/− (medial) to P7+/− (lateral). In the present study we examined the climbing fiber input to the medial half of folium IXcd, the ventral uvula, which spans the medial two stripe pairs (P1+/− to P2+/−). Purkinje cells in the ventral uvula respond to patterns of optic flow resulting from self-motion through the environment along translational axes and their climbing fibers originate in the lateral half of the medial column in the inferior olive (mcIO). Using anterograde injections into this region of the mcIO, we found the following topographic relationship: climbing fibers from the caudal lateral mcIO were located in P1+ and medial P1− ZII stripes; climbing fibers from the rostral lateral mcIO were located in lateral P2+ and P2− ZII stripes, and climbing fibers from the middle lateral mcIO were located in lateral P1− and medial P2+ ZII stripes. These data complement our previous findings showing a topographic relationship between Purkinje cell responses to optic flow visual stimuli and ZII stripes. Taken together, we suggest that a ZII+/− stripe pair may represent a functional unit in the pigeon vestibulocerebellum. J. Comp. Neurol. 522:3629–3643, 2014.

© 2014 Wiley Periodicals, Inc.

The cerebellum is organized into a series of parasagittal zones (Voogd and Bigaré, 1980); this parasagittal architecture can be revealed by climbing fiber (CF) and mossy fiber afferent input, Purkinje cell efferent projections, and Purkinje cell response properties (Llinas and Sasaki, 1989; de Zeeuw et al., 1994; Voogd and Glickstein, 1998; Wu et al., 1999; Ruigrok, 2003; Apps and Garwicz, 2005). Several molecular markers also show a parasagittal expression pattern in the cerebellum (for a review, see Sillitoe and Hawkes, 2013). By far the most extensively examined of these is zebrin II (ZII). The ZII antibody recognizes the 36-kDa isoenzyme aldolase C, which is expressed by Purkinje cells (Brochu et al., 1990; Ahn et al., 1994; Hawkes and Herrup, 1995) in a pattern that is common to several mammalian and avian species (Hawkes, 1992; Hawkes and Herrup, 1995; Sanchez et al., 2002; Pakan et al., 2007; Iwaniuk et al., 2009; Marzban et al., 2010; Marzban and Hawkes, 2011). This organizational similarity across a range of species suggests that the role of ZII is highly conserved, and is likely critical for fundamental cerebellar function. Important aspects of how ZII stripes relate to functional zones within the cerebellum have been investigated, especially in mammals (for examples, see

Figure 1. Zebrin II (ZII) organization and optic flow zones in the vestibulocerebellum in pigeons. A coronal section through folia IXcd and X is depicted, with the ZII stripes, numbered P1 to P7 (medial to lateral) from the midline (thick dashed line). ZII+ Purkinje cells are indicated in red and ZII− Purkinje cells are indicated in pink. P1− is divided into medial and lateral portions by a small satellite immunopositive band 1–2 Purkinje cells wide in the middle of P1− denoted "?". P2+ is divided into medial and lateral portions by a small immunonegative "notch" in the middle of P2+. Across the extent of folium IXcd, Purkinje cells respond to patterns of optic flow resulting from self-motion (as indicated by the spherical flow-diagrams). In medial folium IXcd (the ventral uvula): 1) contraction Purkinje cells are found in P1+ and P1-med; 2) expansion and ascent Purkinje cells are located in P1-lat and P2+med; and 3) descent Purkinje cells are located in P2+lat and P2−. Cells responsive to patterns of optic flow resulting from self-rotation (rVA and rH45 zones) are located laterally in folium IXcd. Scale bar = 400 μm.

Chockkan and Hawkes, 1994; Hallem et al., 1999; Voogd et al., 2003; Sugihara and Shinoda, 2004, 2007; Voogd and Ruigrok, 2004; Pijpers et al., 2006; Sugihara et al., 2007). However, the cerebellum is a highly interconnected and diverse brain region with many functions, and many questions remain regarding the underlying organizational principles in the cerebellum and the specific role that ZII plays in this regard.

Toward this, we use the pigeon vestibulocerebellum (folia IXcd and X) as a model to study the relationships between ZII expression, anatomical connections, and cerebellar function. This model system is ideal to investigate the correspondence of various principles of compartmentalization due to the fact that the functional zonal organization of the pigeon vestibulocerebellum has been extensively documented. For instance, as shown in Figure 1, the specific pattern of ZII expression in this region is known in birds: while folium X (also known as the nodulus) contains homogenously ZII+ Purkinje cells, folium IXcd (comprising the ventral uvula, medially, and the flocculus, laterally) consists of a series of seven marked ZII+/− stripe pairs designated P1+/− through P7+/− (Pakan et al., 2007; Marzban et al., 2010).

In addition, the pattern of Purkinje cell complex spike activity in response to optic-flow stimuli are also well established in the vestibulocerebellum (e.g., Wylie and Frost 1991, 1999; Graham and Wylie, 2012). Optic flow

is a term used by Gibson (1954) to describe the pattern of visual motion that occurs across the entire retina as an organism moves ("self-motion") through an environment consisting of stationary objects and surfaces. Optic flow contrasts with "local" motion, which is due to objects moving across a stationary background (Frost et al., 1990). The pattern of optic flow depends on the specific type of self-motion that occurs. As shown in Figure 1, these patterns can be illustrated as flow-diagrams projected onto a sphere surrounding an animal, where the arrows represent the direction (or "flow") of visual stimuli across the retina of the organism. Self-motion can be divided into two functionally distinct categories, either self-rotation (i.e., rotation of the head relative to the world) or self-translation (i.e., moving from point A to B in the environment). During self-rotation, the optic flow rotates in the direction opposite to the head motion, and there would be circular optic flow about the axis of rotation. For example, rotation about the vertical axis of the head in the leftward direction results in rightward optic flow on the equator of the sphere, and circular motion on the pole of the sphere (see "rVA" flow-diagrams above the flocculus of Fig. 1). During self-translation, in the direction in which the organism is moving there is a "focus of expansion," a point from which the visual flow radiates outward. On the opposite end of the sphere would be a "focus of contraction," a point to which the optic flow

converges. For example, if the organism is moving forward, there is a focus of expansion is in front of them and a focus of contraction directly behind (see the "expansion" flow-diagram shown in purple in Fig. 1).

Specific pathways from the accessory optic system to the vestibulocerebellum are involved in the processing of optic flow stimuli that results from self-motion (Simpson, 1984). Retino-recipient nuclei in the pretectum and the accessory optic system send visual projections to the medial column of the inferior olive (mcIO; Arends and Voogd, 1989), which then carries visual optic flow information to the vestibulocerebellum via CFs (Clarke, 1977; Brecha et al., 1980; Gamlin and Cohen, 1988; Wylie et al., 1997; Wylie, 2001). As illustrated in Figure 1, the specific Purkinje cell complex spike activity in response to patterns of optic flow is highly organized into parasagittal zones in the vestibulocerebellum. In the flocculus, the complex spike activity of Purkinje cells responds to patterns of optic flow resulting from self-rotation. There are two types of rotational neurons: rVA neurons respond to rotation about a vertical axis, whereas rHA neurons respond to rotation about a horizontal axis oriented 45° to the midline (Wylie and Frost, 1993; see also Graf et al., 1988). Complex spike activity in the ventral uvula responds to optic flow resulting from self-translation (Wylie et al., 1993, 1998; Wylie and Frost, 1999). There are four response types: contraction, expansion, descent, and ascent.

In the flocculus, rVA and rHA neurons are organized into four zones: two rVA zones interdigitated with two rHA zones (see Fig. 1; Pakan et al., 2005). The rVA and rHA zones receive input from the caudomedial and rostromedial regions of the mcIO, respectively (Lau et al., 1998; Wylie et al., 1999; Winship and Wylie, 2001). Pakan and Wylie (2008) showed that injections in the caudomedial mcIO resulted in CF labeling restricted to the P4+/− and P6+/− stripe pairs, whereas injections in the rostromedial mcIO resulted in CF labeling restricted to the P5+/− and P7+/− stripe pairs. These data suggested that a ZII+/− pair represents a functional unit in the vestibulocerebellum. This was reinforced by Pakan et al. (2011), who recorded complex spike activity in the flocculus, marked rVA and rHA recording sites with fluorescent dyes, and subsequently processed coronal sections for ZII. They found that rVA Purkinje cells were localized to the P4+/− and P6+/− stripe pairs, whereas rHA Purkinje cells were localized to the P5+/− and P7− stripes (Fig. 1).

Using the same methods as Pakan et al. (2011) described above, we (Graham and Wylie, 2012) showed that the response types in the ventral uvula are topographically organized with respect to the ZII stripes as follows: Purkinje cells responsive to *contraction* were located in the P1+ stripe and the medial half of P1− (P1-med); *descent* Purkinje cells were located in the lateral half of the P2+ stripe (P2+lat) and the P2− stripes. Both *expansion* and *ascent* Purkinje cells were confined to the lateral portion of P1− (P1-lat) and the medial portion of P2+ (P2+med). In the present study, we aimed to determine the direct relationship between climbing fiber projections to the ventral uvula, which arises from the lateral mcIO (Crowder et al., 2000; Winship and Wylie, 2001), and the ZII expression pattern. We made small injections of the anterograde tracer biotinylated dextran amine (BDA) into discrete regions of the lateral mcIO, and examined the resulting olivocerebellar CF labeling in relation to the ZII expression pattern in the ventral uvula. This present study represents the fourth study showing a direct relationship between optic flow zones, ZII expression, and CF input in folium IXcd (Pakan and Wylie, 2008; Pakan et al., 2011; Graham and Wylie, 2012).

MATERIALS AND METHODS
Surgical and tracer injection procedure

The methods reported herein conformed to the guidelines established by the Canadian Council on Animal Care and were approved by the Biosciences Animal Care and Use Committee at the University of Alberta. Ten Silver King and Homing pigeons (*Columba livia*), obtained from a local supplier, were anesthetized with an injection (i.m.) of a ketamine (65 mg/kg) / xylazine (8 mg/kg) cocktail. Supplemental doses were administered as necessary. Animals were placed in a stereotaxic device with pigeon ear bars and a beak bar adapter so that the orientation of the skull conformed to the atlas of Karten and Hodos (1967). To access the inferior olive, bone and dura were removed from the dorsomedial surface of the cerebellum, lateral to the mid-sagittal sinus. The intent was to make localized injections into the regions of the mcIO that provide CF input to the ventral uvula and nodulus. The pigeon inferior olive is divided into ventral and dorsal lamellae, which are conjoined medially by the mcIO (Arends and Voogd, 1989). The rostrocaudal extent of the mcIO ranges from about 1.4–1.8 mm in length. Our previous work showed the lateral half of the mcIO projects to the ventral uvula and nodulus, whereas the medial half of the mcIO projects to the flocculus (Lau et al., 1998; Wylie et al., 1999; Crowder et al., 2000). Furthermore, a single unit recording study of the lateral mcIO showed a topography: contraction neurons were found most caudally, descent neurons were found most rostrally,

and expansion and ascent neurons were found in the middle of the rostrocaudal extent of the lateral mcIO (Winship and Wylie, 2001). To ensure that we were in the desired olivary subnuclei, single-unit extracellular recordings were used to confirm the location of the injection sites. To record the activity of optic flow units in the mcIO, glass micropipettes filled with 2 M NaCl, with tip diameters of 4–5 μm, were advanced through the cerebellum and into the brainstem using a hydraulic microdrive (Frederick Haer, Millville, NJ). Extracellular signals were amplified, filtered, and fed to a window discriminator. Inferior olivary units are easily identified based on their characteristically low firing rate (∼1 spike/s) and proximity to the base of the brain. Upon isolation of a unit in the lateral mcIO, the optic flow preference of the unit was qualitatively determined. The direction-selectivity of the olivary neuron was determined by moving a large (90 × 90°) handheld visual stimulus, consisting of black bars, wavy lines, and dots on a white background, in the receptive field of the unit. With such stimuli, contraction, expansion, ascent, and descent neurons can be easily determined (Winship and Wylie, 2001; Graham and Wylie, 2012). Once the desired area was isolated, the recording electrode was replaced with a micropipette (tip diameter 20–30 μm) containing fluorescent BDA; either mini-ruby (red; D-3312) or mini-emerald (green; D-7178; 10,000 molecular weight; Invitrogen, Carlsbad, CA). The tracers (0.01–0.05 μl of 10% solution in 0.1 M phosphate buffer) were pressure-injected using a Picospritzer II (General Valve, Fairfield, NJ). After surgery the craniotomy was filled with bone wax and the wound was sutured. Birds were given an injection of buprenorphine (0.012 mg/kg, i.m.) as an analgesic.

After a recovery period of 3–5 days the animals were deeply anesthetized with sodium pentobarbital (100 mg/kg) and immediately transcardially perfused with phosphate-buffered saline (PBS; 0.9% NaCl, 0.1 M phosphate buffer) followed by 4% paraformaldehyde in 0.1 M PBS (pH 7.4). The brain was extracted from the skull and immersed in paraformaldehyde for 7 days at 4°C. The brain was then embedded in gelatin and cryoprotected in 30% sucrose in 0.1 M PBS overnight. Using a microtome, frozen serial sections in the coronal plane (40 μm thick) were collected throughout the rostrocaudal extent of the cerebellum and the brainstem.

Immunohistochemistry

ZII expression was visualized using established immunohistochemical techniques described previously (Pakan et al., 2007). Briefly, tissue sections were rinsed thoroughly in 0.1 M PBS and blocked with 10% normal donkey serum (Jackson Immunoresearch Laboratories, West Grove, PA) and 0.4% TritonX-100 in PBS for 1 hour. Tissue was then incubated in PBS containing 0.1% TritonX-100 and the primary antibody, mouse monoclonal anti-zebrin II (1:200 dilution; kindly provided by Richard Hawkes, University of Calgary; Brochu et al., 1990 RRID:AB_10013580) for 60–75 hours at room temperature. Sections were then rinsed in PBS and incubated in a fluorescent secondary; either Cy2 or Cy3 conjugated donkey antimouse antibody (Jackson Immunoresearch Laboratories: diluted 1:100 in PBS, 2.5% normal donkey serum, and 0.4% TritonX-100) for 2 hours at room temperature. The tissue was then rinsed in PBS and mounted onto gelatinized slides for viewing.

Antibody Table:

Name	Immunogen	Details
Anti-Zebrin II	produced by immunization with a crude cerebellar homogenate from the weakly electric fish Apteronotus (Brochu et al.,1990)	Provided by Dr. Richard Hawkes, University of Calgary; raised in mouse; monoclonal. RRID:AB_10013580

Antibody characterization

Anti-zebrin II is a monoclonal antibody grown in mouse, produced by immunization with a crude cerebellar homogenate from the weakly electric fish Apteronotus (Brochu et al., 1990), and recognizes in mouse a single polypeptide band with an apparent molecular weight of 36 kDa, which cloning studies have shown to be the metabolic isoenzyme aldolase C (Ahn et al., 1994; Hawkes and Herrup, 1995). Anti-zebrin II western blot analysis of homogenate of pigeon cerebellum also detects a single immunoreactive polypeptide band, identical in size to the band detected in extracts from the adult mouse cerebellum (Pakan et al., 2007). It was

---

Abbreviations

BDA	Biotinylated dextran amine	P2+lat	Lateral half of P2+
CF	Climbing fiber	P2+med	Medial half of P2+
IXab	Folium IXab of the cerebellum	rHA	Rotation about a horizontal axis
IXcd	Folium IXcd of the cerebellum	rVA	Rotation about the vertical axis
mcIO	Medial column of the inferior olive	X	Folium X of the cerebellum
P1+/−	todesignated zebrin II-immunopositive, -immunonegative zones	ZII+/−	Zebrin II-immunopositive, -immunonegative
P7+/−		?	Zebrin II-immunopositive satellite zone in the middle of P1-
P1-lat	Lateral half of P1−		
P1-med	Medial half of P1−		
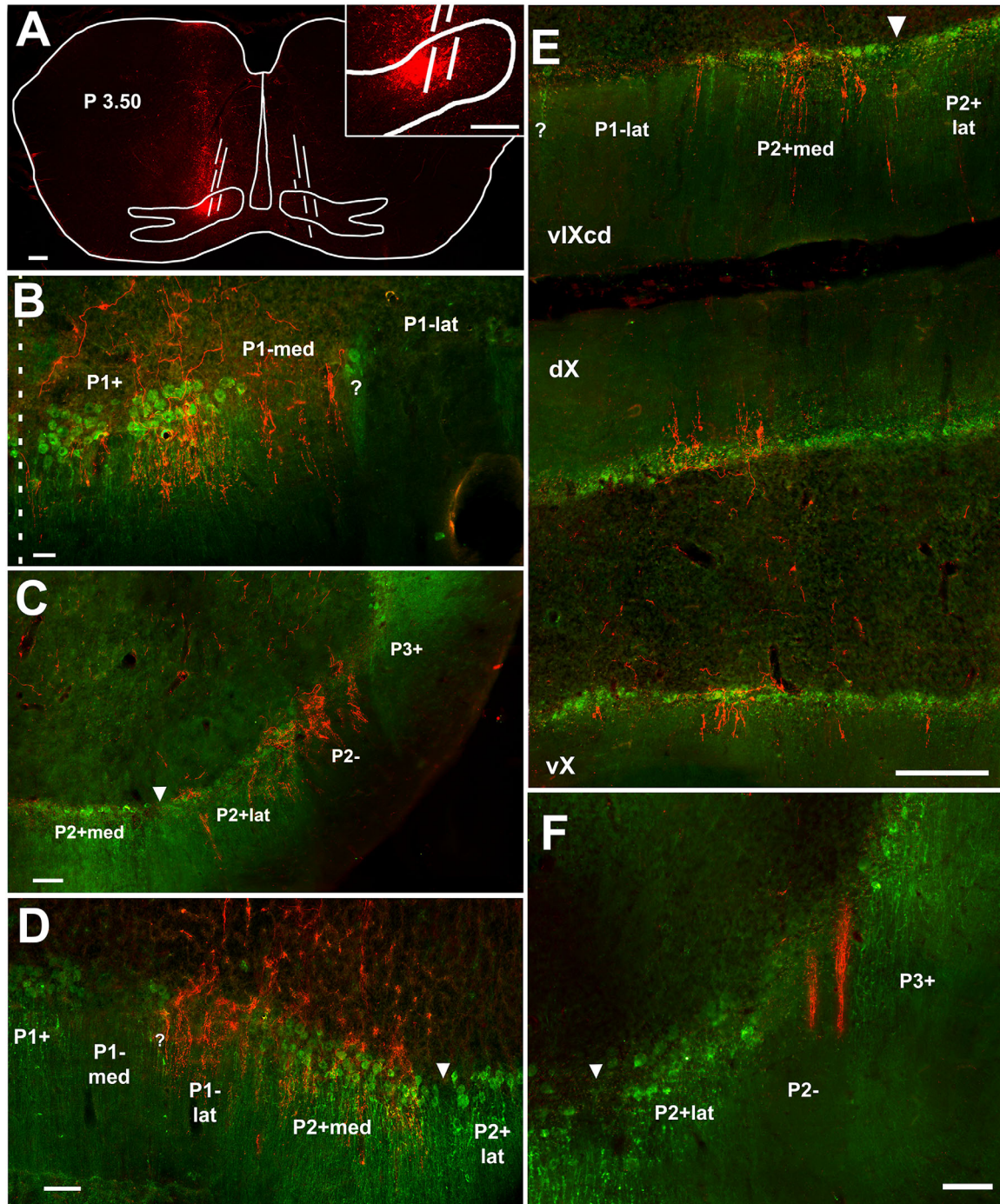
Figure 2. Olivary injection site, CF labeling, and ZII immunohistochemistry in medial folium IXcd. **A:** Photomicrograph of a coronal section through the brainstem and a red-BDA injection in the middle (expansion/ascent) region of the lateral medial column of the inferior olive (mcIO) from case ZIO16. P 3.50 refers to the rostrocaudal location of the section in the stereotaxic atlas of the pigeon brain (Karten and Hodos, 1967). The inferior olive is outlined in white; vertical lines through the mcIO indicate the fibers of the twelfth cranial nerve. The inset in the top right corner shows a higher magnification image of this injection site, illustrating the specific size and location within the mcIO. **B–F:** Photomicrographs of coronal sections through ventral folium IXcd. The molecular layer is represented ventrally, while the Purkinje cell layer and the granule layer are located dorsally. B,C: Typical BDA labeled CFs from case ZIO2 (contraction region) and ZIO6 (descent region), respectively. The dotted line in B represents the midline. D: Red BDA labeled CFs in green immunolabeled ZII zones P1-lat and P2+med from case ZIO5 (expansion/ascent region). E: Red BDA labeled fibers in ZII zones P1-lat and P2+med of folium IXcd with subjacent labeling in folium X from case ZIO17 (expansion/descent region). F: Red BDA labeled CFs on the lateral edge of P2− that do not extend into P3+ from case ZIO16 (descent region). Inverted triangles in (C–F) denote ZII immunonegative "notch" separating P2+ into medial and lateral halves. Scale bars = 200 µm in A, A inset, E; 50 µm in B; 100 µm in C,D,F. See Supplementary Figure 1 for magenta-green version of this figure.
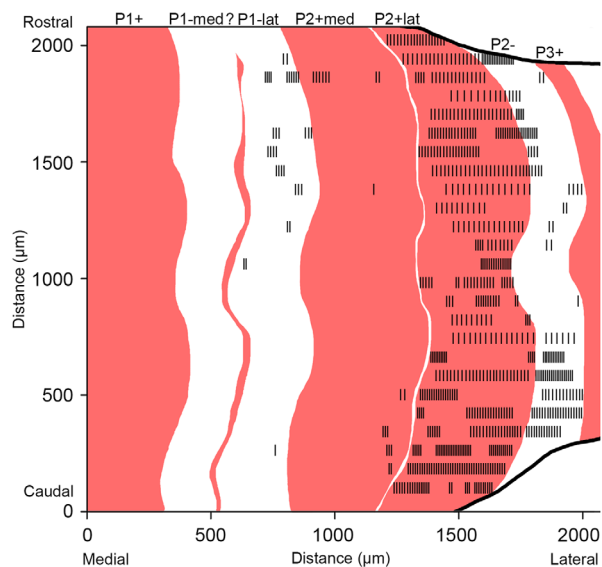
Figure 3. Reconstruction of CF projections and ZII expression in medial folium IXcd from case ZIO6. Black lines represent individual CFs labeled in 25 serial coronal sections (40 µm thick and 40 µm apart) throughout the rostrocaudal extent of the ventral folium of the uvula. In this case, an injection of red BDA was made in the rostral mcIO (descent region). ZII+ zones (in red) are interdigitated by ZII− zones (in white) in the mediolateral plane (x-axis).

used directly from spent hybridoma culture medium diluted 1:200 and labeled a subset of Purkinje cell soma and dendrites in the cerebellum (Fig. 2) as previously reported (Pakan et al., 2007).

Microscopy and data analysis

Sections were viewed with a compound light microscope (Leica DMRE) equipped with the appropriate fluorescence filters (rhodamine and FITC). Images were acquired using a Retiga EXi FAST Cooled mono 12-bit camera (Qimaging, Burnaby, BC) and analyzed with OPENLAB imaging software (Improvision, Lexington MA; RRID:rid_000096). Adobe Photoshop (San Jose, CA) was used to adjust brightness and contrast.

For each injection site the injection core was defined as the area where the BDA tracer was saturated in the tissue and clearly visible, whereas injection penumbra was defined as the area where residual fluorescence around the core could be seen but was devoid of saturated BDA tracer. These were measured using the measurement tool within the OPENLAB imaging software.

Quantitative analysis of the resulting CF labeling throughout the ventral uvula after BDA injections was collected by counting the CFs within a given zone in five serial sections (40 µm thick; 40 µm apart) from

each case, and measuring the size of each ZII zone as well as the location of the counted CFs within each section. From these data, we calculated the average size of each ZII zone, as well as the number of CFs within each ZII zone per 100µm from all cases (see results in Fig. 4). In some instances, qualitative descriptions of the resulting CF labeling are used to describe the extent of labeling in individual cases (i.e., substantial or sparse). These qualitative descriptions are related to the quantitative data described above where heavy/substantial labeling refers to >7.0 CFs counted per 100 µm, moderate labeling refers to between 3.6–7.0 CFs counted per 100 µm, and light/sparse labeling refers to 1.0–3.5 CFs counted per 100 µm. All measurements were made using the measurement tool within the OPENLAB imaging software.

To reconstruct the location and distribution of CFs (Fig. 3) coronal images were taken (with a 20× objective) of the entire folium and a large high-resolution composite was made of each section. Each horizontal row of black lines in the reconstruction represents a single tissue section (40 µm thick) equally spaced throughout the ventral uvula (therefore, for Fig. 3, 25 sections were imaged, counted, and reconstructed). Each CF was then marked with a black line on a layer directly overlaying the images (using Adobe Photoshop) and each corresponding boundary of ZII expression was also marked. The 25 sections were then reconstructed through the rostral-caudal extent and the boundaries of the ZII zones extrapolated; the result is similar to a sampling of CF labeling that would be evident if one were viewing the folia as sliced in the horizontal plane. The reconstruction is therefore a sampling of 25 sections throughout the rostral-caudal extent of the folia and does not represent the entire labeled CF population per case, but rather gives a representation of the distribution of labeling in relation to the ZII stripes throughout the extent of the ventral uvula. Each horizontal row of black lines in the figure, however, does represent an accurate count of CFs per (40 µm thick) section counted.

RESULTS
Climbing fiber labeling in the ventral uvula and nodulus

The results are based on observations in 10 animals, where injections of red and/or green fluorescent BDA were made into the mcIO (Table 1). In nine animals, a single injection of red BDA was made in the mcIO: 1) in two of these cases, the injections were aimed at the caudal mcIO (contraction region; cases ZIO2 and ZIO11); 2) in three of these cases, the injections were
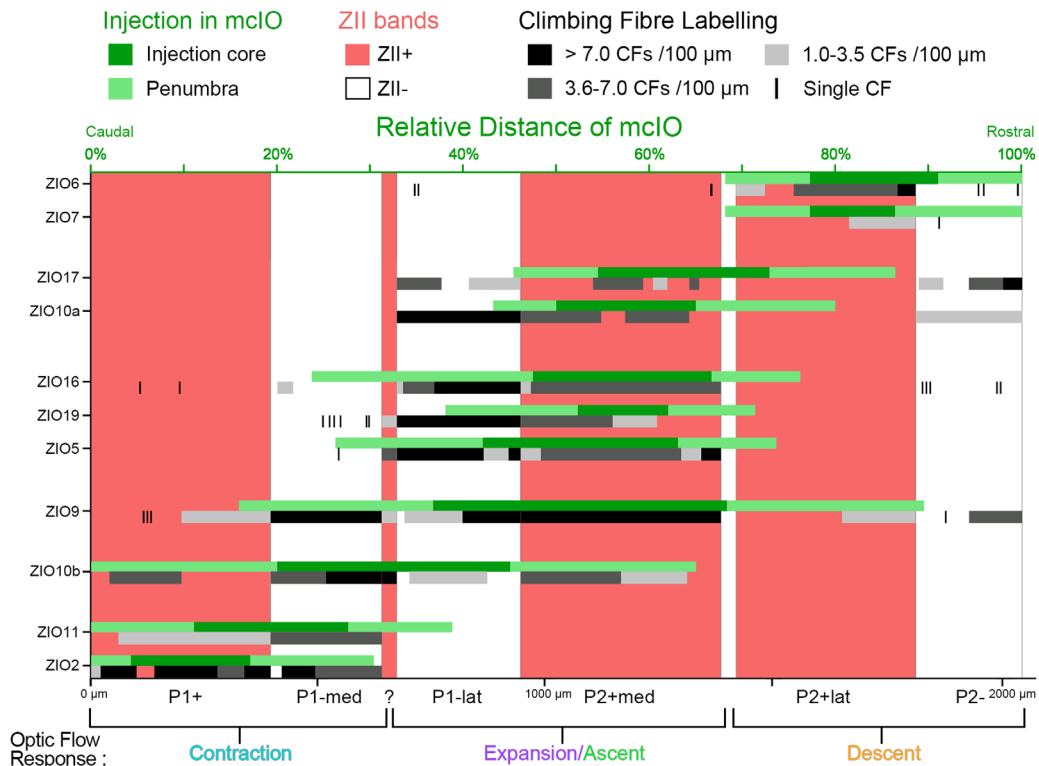
Figure 4. Location and extent of the injections sites in the mcIO and the resulting CF labeling in the ventral lamella of medial folium IXcd. Each case is indicated on the y-axis. There are two bar graphs for each case: 1) the bottom bar graph represents the location of CF labeling in the ZII zones (which are indicated by the bottom x-axis) and the degree of CF labeling (which is indicated by the legend above) from the specified case. The reconstructions of the CF counts from each case were averaged from five serial sections (40 μm thick and 40 μm apart); 2) the top bar graph represents the location and size of each injection expressed as a proportion of the rostrocaudal extent of the mcIO (which are indicated on the top x-axis, and the legend above). The caudal and rostral borders of mcIO are designated 0% and 100%, respectively. The bracketed regions at the bottom of the figure indicate the optic flow preference associated with the mcIO injection site (see also Table 1) and the Purkinje cell complex spike activity in the respective ZII stripes (Graham and Wylie, 2012). Single injections of red BDA were made in all cases except for ZIO10, where red BDA was injected more caudally (ZIO10b), and green BDA was injected more rostrally (ZIO10a).

aimed at the rostral mcIO (descent region; cases ZIO6, ZIO7, and ZIO17); 3) and in four of these cases, the injections were aimed in the middle of the mcIO (expansion and ascent region; cases ZIO5, ZIO9, ZIO16, and ZIO19). One animal (case ZIO10) received two injections: a red injection was aimed into the caudal mcIO (ZIO10b) and a green injection was aimed into the rostral mcIO (ZIO10a). Figure 2A shows a photomicrograph of a representative injection site from case ZIO16, illustrating a red BDA injection in the lateral mcIO. The resulting CF labeling from the BDA injections was entirely contralateral in all cases, robust, and easily distinguishable in the molecular layer. In all cases a prominent band of CF labeling that spanned IXcd and X was observed, an example of which can be seen in Figure 2E. Figure 2B–F show representative photomicrographs of CF labeling (red) in relation to the ZII expression pattern (green). As described case-by-case below, there was a clear topographic relationship

between the rostrocaudal location of the injections and the location of the resulting CF labeling in the ZII stripes. Injections in the caudal lateral mcIO (contraction region) resulted in CF labeling in ZII zones P1+ and P1-med (for example, see Fig. 2B). Injections in the rostral lateral mcIO (descent region) resulted in CF labeling in ZII zones P2+lat and P2− (for example, see Fig. 2C and CF reconstruction in Fig. 3). Injections in the middle lateral mcIO (expansion and ascent region) resulted in CF labeling in ZII zones P1-lat and P2+med (for example, see Fig. 2D,E). While many CFs were seen on the very lateral edge of P2−, as shown in Figure 2F, none were observed in ZII zones P3+/− in any of the cases.

Figure 4 summarizes the extent of the injection sites in the lateral mcIO and the corresponding density of CF labeling in ZII stripes in IXcd from all cases. The CF labeling is collapsed from five serial sections in ZII zones P1+ to P2− where the labeling was heaviest

TABLE 1.
Summary of Injections in the Medial Column of the Inferior Olive (mcIO)

	Case	Optic flow preference at injection site	Tracer injected	Rostral-caudal location of center of injection site within mcIO[1]
Rostral	ZIO6	*Descent*	Red BDA	1480 μm
	ZIO7	*Descent*	Red BDA	1440 μm
	ZIO17	*Expansion*	Red BDA	1120 μm
	ZIO19	*Ascent*	Red BDA	960 μm
	ZIO10a	*Expansion*	Green BDA	920 μm
	ZIO16	*Ascent*	Red BDA	920 μm
	ZIO5	*Expansion*	Red BDA	800 μm
	ZIO9	*Expansion*	Red BDA	800 μm
	ZIO10b	*Contraction*	Red BDA	480 μm
	ZIO11	*Contraction*	Red BDA	280 μm
Caudal	ZIO2	*Contraction*	Red BDA	200 μm

[1]Distance from the caudal pole of the medial column of the inferior olive.

from each case. The rostrocaudal extents of the injections expressed as a percentage of the entire mcIO (upper x-axis) are shown as dark green (injection core) and light green (injection penumbra) bars. As indicated in the figure legend, the density of CF labeling is shown as black (most dense), dark gray or light gray (least dense) bars, or single vertical marks (single CFs) superimposed on the ZII+ (red) and ZII− (white) stripes of the ventral uvula.

Injections in the caudal lateral mcIO

There were three injections in the caudal region of the lateral mcIO where contraction neurons were recorded at the injection site (see Table 1; cases ZIO2, ZIO10b, and ZIO11). In cases ZIO2 and ZIO11, the injections were small (260 μm and 240 μm rostrocaudal spread, respectively, of the injection core) and resulted in CF labeling medially in folia IXcd and X. In IXcd, the CFs were confined entirely to ZII zones P1+ and P1-med (Fig. 4). Case ZIO2, which was the most caudal injection (centered at 200 μm from the caudal tip of mcIO; see green bar in Fig. 4), had heavy labeling throughout P1+, with less labeling in P1-med; this is illustrated in Figure 2B. Case ZIO11, where the injection was slightly more rostral (centered at 280 μm from the caudal tip of mcIO) had heavier CF labeling in P1-med than in P1+, with less overall CF labeling than in case ZIO2 (this is summarized in Fig. 4; note the comparison between the black and gray bars for these cases). The injection in case ZIO10b was slightly more rostral to both ZIO2 and ZIO11 (centered at 480 μm from the caudal tip of mcIO) and was quite a bit larger in comparison (400 μm rostrocaudal spread of the injection core). The heaviest labeling occurred in P1-med, with less labeling in P1+ and P2+med, and the lightest labeling in P1-lat (Fig. 4).

Injections in the rostral lateral mcIO

For the two rostralmost injections in the lateral mcIO, descent neurons were recorded (Table 1; cases ZIO7 and ZIO6). These injections were small (160 μm and 240 μm rostrocaudal spread, respectively, of the injection core; see also green bars in Fig. 4) and resulted in CF labeling confined almost exclusively to ZII zones P2+lat and P2− stripes in folium IXcd (Fig. 4), and a band located beneath these in folium X. Case ZIO6, which was the most rostral injection (Fig. 4; 1,480 μm from the caudal tip of mcIO) had heavy CF labeling in P2+lat, but also substantial labeling in P2−, as shown in Figure 2C. There were a few single CF terminals found in both P2+med and P1-lat (see single black lines in Fig. 4). Figure 3 shows the extent of the CF labeling in IXcd for this case, as reconstructed from serial sections. Note that the overwhelming bulk of the labeling was in P2+lat and P2−. Case ZIO7, where the injection was slightly more caudal (1,440 μm from the caudal tip of mcIO), had most CF labeling confined to P2+lat and P2−, although it was heavier in P2+lat.

Injections in the middle of the lateral mcIO

There were six injections into the middle region of the lateral mcIO. At two injection sites ascent neurons were recorded (Table 1; cases ZIO16 and ZIO19), whereas at four injection sites expansion neurons were recorded (Table 1; ZIO17, ZIO10a, ZIO9, and ZIO5). For these cases, the vast majority of the labeled CFs in IXcd was found in the P1-lat and P2+med stripes (see black bars in Fig. 4), and a band located beneath these in folium X. Cases ZIO16 (Fig. 2A) and ZIO19 both had small injections (240 μm and 160 μm rostrocaudal spread, respectively, of the injection core). Case ZIO16 was the more caudal injection of the two (centered at 920 μm from the caudal tip of mcIO) and CF labeling
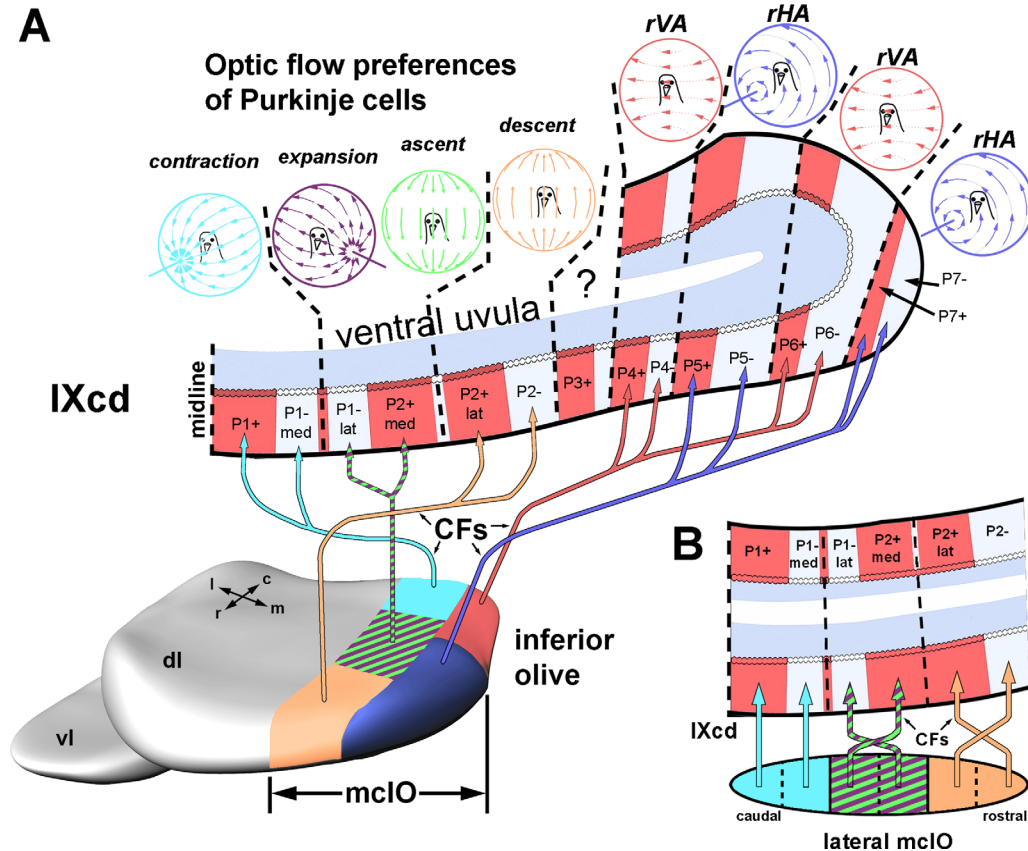
Figure 5. Organization of the pigeon vestibulocerebellum: correlating physiology, anatomy, and intrinsic immunochemistry. **A:** The organization of the zones containing cells responsive to translational optic flow (contraction, expansion, ascent, and descent) and rotational optic flow (rVA and rHA) in relation to climbing fiber (CF) inputs and the expression pattern of zebrin II (ZII) in folium IXcd. ZII-immunopositive (ZII+) Purkinje cells are represented as red, whereas ZII-immunonegative (ZII−) Purkinje cells are white and specific zones are indicated from P1+ to P7−. The visual optic flow preferences of each zone are separated by black dashed lines. Optic flow information reaches folium IXcd as CF inputs from the medial column of the inferior olive (mcIO). The lateral portion of the mcIO contains a contraction region (light blue), an expansion/ascent region (green and purple stripes), and a descent region (orange), whereas the medial portion contains an rVA region (red) and an rHA region (dark blue). All areas of the mcIO project to IXcd via CFs as indicated by the arrows. **B:** The hypothesized caudal-to-rostral projections of the translational optic flow neurons in the lateral mcIO to the ZII+ and ZII− zones in the ventral uvula. C, R, M, and L = caudal, rostral, medial, and lateral; dl and vl = dorsal lamella and ventral lamella of the inferior olive.

was heaviest in P1-lat and quite substantial in P2+med (Fig. 4). There were only a few single CFs observed in each of P1+, P1-med, and P2−. Case ZIO19 (injection centered at 960 μm from the caudal tip of mcIO) was similar: heaviest labeling in P1-lat, substantial labeling in P2+med with only a few single CFs in P1-med (Fig. 4). Case ZIO5 also involved a small injection (240 μm rostrocaudal spread of the injection core), but was located more caudally, centered at 800 μm from the caudal tip of mcIO (green bar in Fig. 4). The resulting CF labeling was confined almost exclusively to P1-lat and P2+med (for example, see Fig. 2D), although slightly heavier in P1-lat (black bar in Fig. 4). There was only a single CFs outside these stripes, in P1-med. The injection in case ZIO10a was also small (240 μm rostrocaudal spread of the injection core), and was centered

at 920 μm from the caudal tip of mcIO (green bar in Fig. 4). The resulting CF labeling was very heavy in ZII zone P1-lat, and substantial in P2+med, with some sparse labeling also seen in P2− (black and gray bars in Fig. 4).

Large injections in mcIO

The injections for the remaining two cases were larger in size. The rostralmost of these injections (ZIO17; centered at 1,120 μm from the caudal tip of mcIO) had a 320 μm rostrocaudal spread of the injection core (green bar Fig. 4). The resulting CF labeling in IXcd was equally abundant in P1-lat, P2+med, and P2− (black and gray bars Fig. 4). Finally, case ZIO9 (centered at 800 μm from the caudal tip of mcIO) had a very large injection (480 μm rostrocaudal spread of

the injection core), and resulted in labeling in every ZII zone in the ventral uvula (Fig 4). Heaviest CF labeling was observed throughout P1-med and P2+med, with fewer CFs occurring in P1-lat and P2−. The sparsest labeling was seen in P1+ and P2+lat.

In summary, as shown in Figure 4, while there is some overlap of CF labeling in cases with injections in different areas of the mcIO, the correspondence of CF labeling and ZII expression is evident: 1) injections into the caudal mcIO (contraction region) resulted in CF labeling in P1+ and P1-med; 2) injections into the middle mcIO (expansion and ascent region) resulted in CF labeling in P1-lat and P2+ med; and 3) injections into the rostral mcIO (descent region) resulted in CF labeling in P2+lat and P2−.

DISCUSSION

Correlating ZII, CFs, and optic flow preferences in the pigeon vestibulocerebellum

In the present study we found that localized injections into physiologically identified regions of the lateral mcIO resulted in labeling largely confined to a ZII+/− stripe pair. Specifically, injections of anterograde tracer into: 1) the caudal lateral mcIO resulted in CFs in P1+ and P1-med; 2) the middle region of the lateral mcIO resulted in CFs in P1-lat and P2+med; and 3) the rostral lateral mcIO resulted in CFs in P2+lat and P2−. Although in some of the cases there was labeling outside of the ZII+/− stripe pair in question, this was minimal in most cases (Figs. 3, 4; cases ZIO5, ZIO6, ZIO10a, ZIO16, ZIO19), or involved larger injections (Fig. 4, cases ZIO9, ZIO10b) where it is likely that injections spanned more than one electrophysiologically distinct region in the lateral mcIO. These findings complement those of Pakan and Wylie (2008), who investigated CF projections from the medial mcIO to the ZII stripes in the pigeon flocculus. They found that CFs from the caudal medial mcIO (rVA region) project to the P4+/− and P6+/− stripe pairs, while CFs from the rostral medial mcIO (rHA region) project to the P5+/− and P7+/− stripe pairs. Furthermore, studies of Purkinje cell complex spike activity in IXcd in response to optic flow stimuli corroborate this organization. Pakan et al. (2011) showed that the complex spike activity of Purkinje cells responsive to rVA optic flow stimulation was confined to P4+/− and P6+/− while the activity of Purkinje cells responsive to rHA optic flow stimulation was confined to P5+/− and P7−. Graham and Wylie (2012) recently showed that Purkinje cells responsive to contraction optic flow was located

most medially in the P1+ and P1-med stripes, while descent Purkinje cells were located most laterally in the P2+lat and P2− stripes. Both expansion and ascent Purkinje cells were confined to the P1-lat and the P2+med stripes. Taken together, these data and results from the current study, summarized in Figure 5A, suggest that a ZII+/− stripe pair represents a functional unit across an entire folium in the pigeon vestibulocerebellum; whether this pattern generalizes to other areas of the avian cerebellum is unknown.

At present, we are uncertain as to the reason that the P1-lat/P2+med stripe pair contains both ascent and expansion neurons. Similarly, we are uncertain as to the function of the P3+/− stripe pair. CFs were not found in P3+/− from any of our injections in the mcIO. Graham and Wylie (2012) found that complex spike activity in P3+ was not modulated in response to visual motion stimuli and suggested that the P3+/− stripe could be equivalent to the C2 zone found in the mammalian flocculus. Complex spike activity in the C2 zone is nonresponsive to optic flow stimulation, and is proposed to be involved in generating head movements (de Zeeuw and Koekkoek, 1997). Alternatively, the P3+/− stripe pair could be a vestibular zone, similar to those described in the uvula/nodulus of rabbits by Barmack and Shojaku (1995).

Climbing fiber input to ZII+ and ZII− stripes

Our finding that a ZII+/− stripe pair receives CF input from a particular region in the inferior olive seems to conflict with mammalian research. Studies in mammals have repeatedly emphasized that an olivary subnucleus projects to either a ZII+ or ZII− stripe, but never both (Gravel et al., 1987; Sugihara and Shinoda, 2004; Apps and Garwicz, 2005; Pijpers et al., 2006; Sugihara and Quy, 2007). For example, Voogd et al. (2003) compared the distribution of olivocerebellar projections to the copula pyramidis and the paramedian lobule with ZII expression patterns in the rat. They showed that, generally, CFs originating from the rostral dorsal accessory olive innervate the ZII− stripes of the C1 and C3 zones, and that the rostral medial accessory olive and principal olive innervate the ZII+ stripes of the C2 and D zones, respectively. Voogd and Ruigrok (2004) also compared parasagittal CF projections to the vermis with ZII stripes in the cerebellum of rats. They showed that discrete injections in various inferior olivary subnuclei resulted in CF bands that corresponded with either a ZII+ or a ZII− stripe, but not both. In a comprehensive study of the entire rat cerebellum, Sugihara and Shinoda (2004) injected BDA into various inferior olive regions and compared the resulting CF labeling with ZII expression. They found that CFs from the principal olive

and areas near to it as well as CFs from several medial subnuclei project to ZII+ zones, while CFs from the centrocaudal portion of the medial accessory olive project to ZII− stripes in the vermis. They also found that the dorsal accessory olive and neighboring regions innervate ZII− and lightly ZII+ stripes in the hemisphere, and the rostral and caudal pars intermedia.

To reiterate, in the present study the efferent projection of a functional region of the mcIO in pigeons was not confined solely to either a ZII+ or a ZII− stripe in the vestibulocerebellum. In fact, a given region of the mcIO projected to a particular ZII+/− pair. However, it is possible that the projections to a ZII+/− stripe pair arise from different neurons, or even separate populations of neurons in a particular region within the mcIO. In fact, a close examination of Figure 4 suggests that the latter may be the case. Figure 5B gives a summary of what we propose would be the subzones in the mcIO that would project to ZII− and ZII+ stripes in folium IXcd. Our most caudal injection in the contraction region of the mcIO (ZIO2) resulted in the heaviest labeling in P1+, while a slightly more rostral injection (ZIO11) resulted in heaviest labeling in P1-med. In the other cases where we saw labeling in P1+ and P1-med (ZIO10b, ZIO9, ZIO5, ZIO19, and ZIO16), labeling was always heavier in P1-med when compared to P1+ (or labeling did not occur at all in P1+, as in cases ZIO5 and ZIO19). This seems to indicate that the region of the mcIO that projects to P1-med is located closer to the expansion/ascent region (i.e., the more rostral portion of the contraction region of the mcIO; Fig. 5B, blue area). Similarly, our most rostral injections into the descent region of the mcIO (ZIO6 and ZIO7) resulted in heavier CF labeling in P2+lat compared to P2−. It is only as mcIO injections move more caudal to this that we see heavier labeling in P2− compared to P2+lat (e.g., ZIO17, ZIO10a, ZIO16, ZIO9). This seems to indicate that the region of the mcIO that projects to P2− is located closer to the expansion/contraction region (i.e., the more caudal portion of the descent region of the mcIO; Fig. 5B, orange area). Finally, upon examination of the injections into the expansion/ascent region, the more rostral injections (ZIO17, ZIO10a, ZIO16, ZIO19) seem to project preferentially to P1-lat compared to P2+med. The more caudal injections either project more heavily to P2+med vs. P1-lat (as in ZIO9) or almost equivalently to both, as in case ZIO5. Also, with our most rostral injection into the contraction region, there is heavier labeling in P2+med than in P1-lat. Thus, it seems to indicate that the region of the mcIO that projects to P1-lat is located more rostrally, while the P2+med projecting area is more caudal within expansion/ascent region (Fig. 5B, green and

magenta stripes). Retrograde studies are needed to confirm these hypotheses.

Other studies correlating function with olivary input to zebrin stripes

Recently, studies have aimed to understand ZII stripes in relation to functional zones in the cerebellum. Voogd et al. (1996) suggested that ZII+ and ZII− bands may have different functional roles as inferior olivary subnuclei project to either ZII+ or ZII− bands and receive input from particular sensory systems. More specifically, Sugihara et al. (2004) postulated that the ZII− stripes receive input from CFs conveying somatosensory information, whereas ZII+ stripes receive input from CFs conveying information from visual, auditory, and other sensory systems (see Voogd et al., 2003; Voogd and Ruigrok, 2004; Sugihara and Quy, 2007; Sugihara and Shinoda, 2007); this pattern of functional input is most convincing in the cerebellar hemispheres. Voogd et al. (1996) provided evidence in support of this hypothesis in the mammalian vestibulocerebellum, showing that the ventral lateral outgrowth, which processes visual-optokinetic information, projects to ZII+ stripes in lobule X and ventral IXcd, while somatosensory olivary subnuclei project to ZII− bands in the dorsal margin of IXcd. However, this theory does not pertain to the pigeon vestibulocerebellum, as we have found in this study that the visual CF inputs from the mcIO clearly project to both ZII+/− stripes and visual climbing fiber responses also span ZII+/− bands (Graham and Wylie, 2012). Furthermore, it appears that the only olivary inputs to the vestibulocerebellum arrive from the mcIO and convey visual information. This is supported by anatomical studies demonstrating that the mcIO receives visual input from retino-recipient nuclei in the pretectum and accessory optic system (Clarke, 1977; Brecha et al., 1980; Gamlin and Cohen, 1988; Wylie et al., 1997; Wylie, 2001), and by electrophysiological studies detailing the responses of neurons in the mcIO to optic flow stimuli (Wylie and Frost, 1993; Winship and Wylie, 2001). Also, somatosensory information, from both ascending (Wild, 1989) and descending systems (Wild and Williams, 2000), reaches the ventral lamella of the IO and not the mcIO.

In mammals, there are exceptions to the correspondence between somatosensory input to ZII+ stripes and other sensory input to ZII− stripes in other cerebellar regions as well. For example, the group beta and the dorsomedial cell column carries vestibular information to ZII+ stripes in lobules VIII–X, but the subnucleus B of the caudal medial accessory olive also carries vestibular information to a ZII− stripe in the

lateral A subzone of the anterior vermis (Gerrits et al., 1985; Voogd and Ruigrok, 2004; Voogd and Barmack, 2006). Although comparative data on these vestibular projections would be very interesting, to date there is no knowledge of vestibular input to the pigeon inferior olive and no known avian homologs of the above-mentioned olivary subnuclei. Another exception, in mammals, involves nuclei at the mesodiencephalic junction that provide the majority of the CFs to ZII+ stripes via the rostral medial accessory olive and the principle olivary nucleus; these nuclei relay information from motor structures, including the parvocellular red nucleus, the nucleus of Darkschewitsch, as well as the prefrontal, eyefield, premotor, motor, and parietal areas (Swenson and Castro, 1983; Onodera, 1984; Holstege and Tan, 1988; de Zeeuw et al., 1989). The subnucleus a, which receives input from the spinal cord, also projects to ZII+ stripes (Matsushita et al., 1991).

Other functional considerations pertaining to zebrin stripes

Although the focus of this study was the pattern of olivary input to the ventral uvula, when considering the functional implications of the pattern of ZII expression it is also important to consider the pattern of mossy fiber input to the ZII stripes in folium IXcd. The parasagittal zonal arrangement of mossy fiber projections is generally broader, with less well-defined borders than CF projection zones; however, a degree of correspondence with ZII stripes has been found in both mammals (Ji et al., 1994; Chockan and Hawkes, 1994; Voogd and Ruigrok, 1997) and birds (Pakan et al., 2010). For example, Pakan et al. (2010) showed that mossy fiber inputs from two retinorecipient nuclei in pigeons that are responsive to optic flow, the pretectal nucleus lentiformis mesencephali (LM) and the nucleus of the basal optic root (nBOR), project preferentially to ZII+ stripes across the mediolateral extent of folium IXcd, including the ventral uvula. Whether there are MF afferents that project preferentially to ZII− Purkinje cells in the pigeon is unknown (for further discussion, see Pakan et al., 2010). Interestingly, it appears that in rats the termination of trigeminal mossy fibers in the uvula are found in the same location as ZII− stripes (Chockkan and Hawkes, 1994; Voogd and Ruigrok, 1997).

The "one-map hypothesis" proposed by Apps and Hawkes (2009) suggests that there may be an alignment (anatomical and physiological) between mossy fiber and climbing fiber projections that target the same Purkinje cell stripes as defined by ZII expression (either ZII+ or ZII−, but not necessarily both). The possibility exists that mossy fiber projections from LM and

nBOR to ZII+ zones in the ventral uvula may correspond to a finer organization of microzones within the larger ZII+/− functional pairs; these larger pairs being defined by their common CF input and physiological response properties. This relationship is potentially more complicated than a one-to-one zonal alignment in the pigeon vestibulocerebellum, as our results suggest that a single mossy fiber zone does not align with the entirety of a single CF zone, but instead aligns only with the ZII+ portion of a single CF zone. However, this does not necessarily contradict the ideas put forth by Apps and Hawkes (2009), as it shows that a *consistent* relationship does exist between the mossy fiber, CF, and ZII stripes (see also Pakan et at., 2010).

There is also a growing body of literature on the physiological properties of the ZII+ and the ZII− stripes in the cerebellum and their relation to information processing (e.g., Wadiche and Jahr, 2005; Gao et al., 2006; Sugihara et al., 2007; Mostofi et al., 2010; Paukert et al., 2010; see Ebner et al., 2012, for review). For example, Paukert et al. (2010) showed that CFs in ZII+ stripes release more glutamate per action potential than CFs in ZII− stripes and proposed that ZII+ Purkinje cells undergo more activity-dependent synaptic plasticity than ZII− Purkinje cells. Additionally, Gao et al. (2006) showed that molecular layer inhibition is organized into inhibitory bands extending across a folium and that these bands are aligned with ZII+ stripes and function to modulate the spatial pattern of cerebellar cortical activity. Interestingly, the excitatory amino acid transporter type 4 (EAAT4) may play a role in this parasagittally organized inhibition (Reinert et al., 2011) and the expression of EAAT4 is congruent with ZII+ stripes (Dehnes et al., 1998). Therefore, ZII+ and ZII− stripes have been shown to respond differentially to CF activity as well as parallel fiber stimulation, including levels of excitability and synaptic plasticity, and these diversities likely underlie distinct functional differences between the ZII+ and ZII− stripes. One must consider, however, that these studies are largely from investigations in the mammalian cerebellar hemispheres and, although mammals and aves share many of the same underlying organizational principles in the cerebellum, generalization to the specific physiological properties of ZII+ versus ZII− stripes in the pigeon cerebellum would need direct examination, and would indeed be interesting from an evolutionary perspective.

Beyond folium IXcd

Although we have concluded that a given CF projection zone spans a ZII+/− stripe pair in folium IXcd, the zone itself obviously continues into folium X (Fig. 2H). Purkinje cells in folium X are all ZII+. It is possible

that other molecular markers are expressed in stripes in X, which may be related to olivary input and the functional zones. For example, in the mouse cerebellum, heatshock protein-25 (Hsp 25) is expressed as parasagittal bands of high and low immunoreactivity in the nodulus and flocculus (Armstrong et al., 2000), areas that are homogenously ZII+. It is not yet known if Hsp 25 is expressed as stripes in the pigeon cerebellum. On the other hand, the ZII stripes extend beyond the optic flow zones. With respect to IXcd, the ZII stripes extend across the dorsal and ventral lamellae, yet the CF inputs and optic flow responses in the uvula are confined (by and large) to the ventral lamella (Wylie et al., 1993; Graham and Wylie, 2012; Fig. 5A). Similarly, the ZII stripes in IXcd are contiguous with those in ventral IXab, and possibly other more dorsal folia (Pakan et al., 2007). If and how Purkinje cells in a given ZII stripe spanning different folia relate functionally remains to be seen.

ACKNOWLEDGMENT

CONFLICT OF INTEREST

The authors have no conflict of interest.

AUTHOR ROLES

All authors had full access to all the data in the study and take responsibility for the integrity of the data and the accuracy of the data analysis. Study concept and design: D.J.G, J.M.P.P, D.R.W. Acquisition of data: D.J.G, J.M.P.P, Analysis and interpretation of data: D.J.G, J.M.P.P, D.R.W. Drafting of the article: D.J.G., J.M.P.P., D.R.W. Critical revision of the article for important intellectual content: D.J.G, J.M.P.P, D.R.W. Statistical analysis: D.J.G. Obtained funding: D.J.G., J.M.P.P, D.R.W. Study supervision: D.R.W.

LITERATURE CITED

Ahn AH, Dziennis S, Hawkes R, Herrup K. 1994. The cloning of zebrin II reveals its identity with aldolase C. Development 120:2081–2090.

Apps R, Garwicz M. 2005. Anatomical and physiological foundations of cerebellar information processing. Nat Rev Neurosci 6:297–311.

Apps R, Hawkes R. 2009. Cerebellar cortical organization: a one-map hypothesis. Nat Rev Neurosci 10:670–681.

Arends J, Voogd J. 1989. Topographic aspects of the olivocerebellar system in the pigeon. Exp Brain Res 17:52–57.

Armstrong CL, Krueger-Naug AM, Currie RW, Hawkes R. 2000. Constitutive expression of the 25-kDa heat shock protein Hsp25 reveals novel parasagittal bands of Purkinje cells in the adult mouse cerebellar cortex. J Comp Neurol 416:383–397.

Barmack NH, Shojaku H. 1995. Vestibular and visual climbing fiber signals evoked in the uvula-nodulus of the rabbit cerebellum by natural stimulation. J Neurophysiol 74:2573–2589.

Brecha N, Karten HJ, Hunt SP. 1980. Projections of the nucleus of the basal optic root in the pigeon: an autoradiographic and horseradish peroxidase study. J Comp Neurol 189:615–670.

Brochu G, Maler L, Hawkes R. 1990. Zebrin II: a polypeptide antigen expressed selectively by Purkinje cells reveals compartments in rat and fish cerebellum. J Comp Neurol 291:538–552.

Chockkan V, Hawkes R. 1994. Functional and antigenic maps in the rat cerebellum: zebrin compartmentation and vibrissal receptive fields in lobule IXa. J Comp Neurol 345:33–45.

Clarke PG. 1977. Some visual and other connections to the cerebellum of the pigeon. J Comp Neurol 174:535–552.

Crowder NA, Winship IR, Wylie DR. 2000. Topographic organization of inferior olive cells projecting to translational zones in the vestibulocerebellum of pigeons. J Comp Neurol 419:87–95.

Dehnes Y, Chaudhry FA, Ullensvang K, Lehre KP, Storm-Mathisen J, Danbolt NC. 1998. The glutamate transporter EAAT4 in rat cerebellar Purkinje cells: a glutamate-gated chloride channel concentrated near the synapse in parts of the dendritic membrane facing astroglia. J Neurosci 18:3606–3619.

de Zeeuw CI, Koekkoek SK. 1997. Signal processing in the C2 module of the flocculus and its role in head movement control. Prog Brain Res 114:299–320.

de Zeeuw CI, Holstege JC, Ruigrok TJ, Voogd J. 1989. Ultrastructural study of the GABAergic, cerebellar, and mesodiencephalic innervations of the cat medial accessory olive: anterograde tracing combined with immunocytochemistry. J Comp Neurol 284:12–35.

de Zeeuw CI, Wylie DR, DiGiorgi PL, Simpson JI. 1994. Projections of individual Purkinje cells of identified zones in the flocculus to the vestibular and cerebellar nuclei in the rabbit. J Comp Neurol 349:428–447.

Ebner TJ, Wang X, Gao W, Cramer SW, Chen G. 2012. Parasagittal zones in the cerebellar cortex differ in excitability, information processing, and synaptic Plasticity. Cerebellum 11:418–419.

Frost BJ, Wylie DR and Wang Y-C. 1990. The processing of object and self-motion in the tectofugal and accessory optic pathways of birds. Vision Res 30:1677–1688.

Gamlin PD, Cohen DH. 1988. Projections of the retinorecipient pretectal nuclei in the pigeon (*Columba livia*). J Comp Neurol 269:18–46.

Gao W, Chen G, Reinert KC, Ebner TJ. 2006. Cerebellar cortical molecular layer inhibition is organized in parasagittal zones. J Neurosci 26:8377–8387.

Gerrits NM, Voogd J, Magras IN. 1985. Vestibular afferents of the inferior olive and the vestibulo-olivo-cerebellar climbing fiber pathway to the flocculus in the cat. Brain Res 332:325–336.

Gibson JJ. 1954. The visual perception of objective motion and subjective movement. Psychol Rev 61:304–314.

Graf W, Simpson JI, Leonard CS. 1988. Spatial organization of visual messages of the rabbit's cerebellar flocculus. II. Complex and simple spike responses of Purkinje cells. J Neurophysiol 60:2091–2121.

Graham DJ, Wylie DR. 2012. Zebrin-immunopositive and -immunonnegative stripe pairs represent functional units in the pigeon vestibulocerebellum. J Neurosci 32:12769–12779.

Gravel C, Eisenman LM, Sasseville R, Hawkes R. 1987. Parasagittal organization of the rat cerebellar cortex: direct correlation between antigenic Purkinje cell bands

revealed by mabQ113 and the organization of the olivo-cerebellar projection. J Comp Neurol 265:294–310.

Hallem JS, Thompson JH, Gundappa-Sulur G, Hawkes R, Bjaalie JG, Bower JM. 1999. Spatial correspondence between tactile projection patterns and the distribution of the antigenic Purkinje cell markers anti-zebrin I and anti-zebrin II in the cerebellar folium crus IIA of the rat. Neuroscience 93:1083–1094.

Hawkes R. 1992. Antigenic markers of cerebellar modules in the adult mouse. Biochem Soc Trans 20:391–395.

Hawkes R, Herrup K. 1995. Aldolase C/zebrin II and the region-alization of the cerebellum. J Mol Neurosci 6:147–158.

Herrup K, Kuemerle B. 1997. The compartmentalization of the cerebellum. Annu Rev Neurosci 20:61–90.

Holstege G, Tan J. 1988. Projections from the red nucleus and surrounding areas to the brainstem and spinal cord in the cat. An HRP and autoradiographical tracing study. Behav Brain Res 28:33–57.

Iwaniuk AN, Marzban H, Pakan JM, Watanabe M, Hawkes R, Wylie DR. 2009. Compartmentation of the cerebellar cortex of hummingbirds (Aves: Trochilidae) revealed by the expression of zebrin II and phospholipase C beta 4. J Chem Neuroanat 37:55–63.

Ji, Z, Hawkes R. 1995. Developing mossy fiber terminal fields in the rat cerebellar cortex may segregate because of Purkinje cell compartmentation and not competition. J Comp Neurol 359:197–212.

Karten H, Hodos W. 1967. A stereotaxic atlas of the brain of the pigeon (Columba livia). Baltimore, MD: Johns Hopkins Press.

Lau KL, Glover RG, Linkenhoker B, Wylie DR. 1998. Topo-graphical organization of inferior olive cells projecting to translation and rotation zones in the vestibulocerebellum of pigeons. Neuroscience 85:605–614.

Llinas R, Sasaki K. 1989. The functional organization of the olivocerebellar system as examined by multiple Purkinje cell recordings. Eur J Neurosci 1:587–602.

Marzban H, Hawkes R. 2011. On the architecture of the pos-terior zone of the cerebellum. Cerebellum 10:422–434.

Marzban H, Chung S-H, Kheradpezhouh M, Watanabe M, Voogd J, Hawkes R. 2010. Antigenic compartmentation of the cerebellar cortex in the chicken (Gallus domesti-cus). J Comp Neurol 518:2221–2239.

Matsushita M, Ragnarson B, Grant G. 1991. Topographic rela-tionship between sagittal Purkinje cell bands revealed by a monoclonal antibody to zebrin I and spinocerebellar projections arising from the central cervical nucleus in the rat. Exp Brain Res 84:133–141.

Mostofi A, Holtzman T, Grout AS, Yeo CH, Edgley SA. 2010. Elec-trophysiological localization of eyeblink-related microzones in rabbit cerebellar cortex. J Neurosci 30:8920–8934.

Onodera S. 1984 Olivary projections from the mesodience-phalic structures in the cat studied by means of axonal transport of horseradish peroxidase and tritiated amino acids. J Comp Neurol 227:37–49.

Pakan JMP, Wylie DR. 2008. Congruence of zebrin II expres-sion and functional zones defined by climbing fiber topography in the flocculus. Neuroscience 157:57–69.

Pakan JMP, Todd KG, Nguyen AP, Winship IR, Hurd PL, Jantzie LL, Wylie DR. 2005. Inferior olivary neurons innervate multiple zones of the flocculus in pigeons (Columba livia). J Comp Neurol 486:159–168.

Pakan JMP, Iwaniuk AN, Wylie DR, Hawkes R, Marzban H. 2007. Purkinje cell compartmentation as revealed by zebrin II expression in the cerebellar cortex of pigeons (Columba livia). J Comp Neurol 501:619–630.

Pakan JMP, Graham DJ, Wylie DR. 2010. Organization of visual mossy fiber projections and zebrin expression in the pigeon vestibulocerebellum. J Comp Neurol 518:175–198.

Pakan JMP, Graham DJ, Gutiérrez-Ibáñez C, Wylie DR. 2011. Organization of the cerebellum: correlating zebrin immu-nochemistry with optic flow zones in the pigeon floccu-lus. Vis Neurosci 28:163–174.

Paukert M, Huang YH, Tanaka K, Rothstein JD, Bergles DE. 2010 Zones of enhanced glutamate release from climb-ing fibers in the mammalian cerebellum. J Neurosci 30: 7290–7299.

Pijpers A, Apps R, Pardoe J, Voogd J, Ruigrok TJ. 2006. Pre-cise spatial relationships between mossy fibers and climbing fibers in rat cerebellar cortical zones. J Neurosci 26:12067–12080.

Reinert KC, Gao W, Chen G, Wang X, Peng Y, Ebner TJ. 2011. Cellular and metabolic origins of flavoprotein autofluores-cence in the cerebellar cortex in vivo. Cerebellum 10: 585–599.

Ruigrok TJ. 2003. Collateralization of climbing and mossy fibers projecting to the nodulus and flocculus of the rat cerebellum. J Comp Neurol 466:278–298.

Sanchez M, Sillitoe RV, Attwell PJ, Ivarsson M, Rahman S, Yeo CH, Hawkes R. 2002. Compartmentation of the rabbit cerebellar cortex. J Comp Neurol 444:159–173.

Sillitoe RV, Hawkes R. 2013. Zones and stripes: development of cerebellar topography. In: Manto M, Gruol D, Schmahmann J, Koibuchi N, Rossi F, editors. Handbook of cerebellum and cerebellar disorders. New York: Springer. p 43–59.

Simpson JI. 1984. The accessory optic system. Annu Rev Neu-rosci 7:13–41.

Sugihara I, Quy PN. 2007. Identification of aldolase C com-partments in the mouse cerebellar cortex by olivocere-bellar labeling. J Comp Neurol 500:1076–1092.

Sugihara I, Shinoda Y. 2004. Molecular, topographic, and functional organization of the cerebellar cortex: a study with combined aldolase C and olivocerebellar labeling. J Neurosci 24:8771–8785.

Sugihara I, Shinoda Y. 2007. Molecular, topographic, and functional organization of the cerebellar nuclei: analysis by three-dimensional mapping of the olivonuclear projec-tion and aldolase C labeling. J Neurosci 27:9696–9710.

Sugihara I, Ebata S, Shinoda Y. 2004. Functional compartmen-talization in the flocculus and the ventral dentate and dorsal group y nuclei: an analysis of single olivocerebel-lar axonal morphology. J Comp Neurol 470:113–133.

Sugihara I, Marshall SP, Lang EJ. 2007. Relationship of com-plex spike synchrony bands and climbing fiber projection determined by reference to aldolase C compartments in crus IIa of the rat cerebellar cortex. J Comp Neurol 501: 13–29.

Swenson RS, Castro AJ. 1983. The afferent connections of the inferior olivary complex in rats. An anterograde study using autoradiographic and axonal degeneration techni-ques. Neuroscience 8:259–275.

Voogd J, Barmack NH. 2006. Oculomotor cerebellum. Prog Brain Res 151:231–268.

Voogd J, Bigaré F. 1980. Topographical distribution of olivary and cortico nuclear fibers in the cerebellum: a review. New York: Raven Press.

Voogd J, Gerrits NM, Ruigrok TJ. 1996. Organization of the vestibulocerebellum. Ann N Y Acad Sci 781:553–579.

Voogd J, Glickstein M. 1998. The anatomy of the cerebellum. Trends Neurosci 21:370–375.

Voogd J, Ruigrok TJ. 2004. The organization of the corticonu-clear and olivocerebellar climbing fiber projections to the rat cerebellar vermis: the congruence of projection zones and the zebrin pattern. J Neurocytol 33:5–21.

Voogd J, Pardoe J, Ruigrok TJ, Apps R. 2003. The distribution of climbing and mossy fiber collateral branches from the copula pyramidis and the paramedian lobule: congruence of climbing fiber cortical zones and the pattern of zebrin banding within the rat cerebellum. J Neurosci 23:4645–4656.

Wadiche JI, Jahr CE. 2005. Patterned expression of Purkinje cell glutamate transporters controls synaptic plasticity. Nat Neurosci 8:1329–1334.

Wild JM. 1989. Avian somatosensory system. II Ascending projections of the dorsal column and external cuneate nuclei in the pigeon. J Comp Neurol 287:1–18.

Wild JM, Williams MN. 2000. Rostral wulst in passerine birds. I. Origin, course, and terminations of an avian pyramidal tract. J Comp Neurol 416:429–450.

Winship IR, Wylie DR. 2001. Responses of neurons in the medial column of the inferior olive in pigeons to translational and rotational optic flowfields. Exp Brain Res 141:63–78.

Wu HS, Sugihara I, Shinoda Y. 1999. Projection patterns of single mossy fibers originating from the lateral reticular nucleus in the rat cerebellar cortex and nuclei. J Comp Neurol 411:97–118.

Wylie DR. 2001. Projections from the nucleus of the basal optic root and nucleus lentiformis mesencephali to the inferior olive in pigeons (Columba livia). J Comp Neurol 429:502–513.

Wylie DR, Frost BJ. 1991. Purkinje cells in the vestibulocerebellum of the pigeon respond best to either translational or rotational wholefield visual motion. Exp Brain Res 86:229–232.

Wylie DR, Frost BJ. 1993. Responses of pigeon vestibulocerebellar neurons to optokinetic stimulation. II. The 3-dimensional reference frame of rotation neurons in the flocculus. J Neurophysiol 70:2647–2659.

Wylie DR, Frost BJ. 1999. Complex spike activity of Purkinje cells in the ventral uvula and nodulus of pigeons in response to translational optic flow. J Neurophysiol 81:256–266.

Wylie DR, Kripalani T, Frost BJ. 1993. Responses of pigeon vestibulocerebellar neurons to optokinetic stimulation. I. Functional organization of neurons discriminating between translational and rotational visual flow. J Neurophysiol 70:2632–2646.

Wylie DR, Linkenhoker B, Lau KL. 1997. Projections of the nucleus of the basal optic root in pigeons (Columba livia) revealed with biotinylated dextran amine. J Comp Neurol 384:517–536.

Wylie DRW, Bischof WF, Frost BJ. 1998. Common reference frame for the coding translational and rotational optic flow. Nature 392:278–282.

Wylie DR, Winship IR, Glover RG. 1999. Projections from the medial column of the inferior olive to different classes of rotation-sensitive Purkinje cells in the flocculus of pigeons. Neurosci Lett 268:97–100.